Defence Science Journal, Vol. 57, No. 4, July 2007, pp. 417-424

Infrared Extinction Coefficients of Artificial Aerosol

Jiachun Wang, Jiaming Shi, Jiayin Wang, Yongshun Ling and Xu Bo
Hefei Institute of Electronic Engineering, Hefei 230 037, People's Republic of China

ABSTRACT

The artificial aerosol is widely used in the modern battlefields to protect the potential targets and to conceal the movement of personnel and materials. In this paper, the double-band infrared extinction coefficients of the artificial aerosol have been calculated and compared with the experimental data. The particulates were assumed to be small spheres and Mie's theory was employed with the grain size distribution function being lognormal. The numerical and the experimental results show that the size distribution and the materials of the particles are decisive of their infrared extinction capability.

Keywords: Infrared, extinction, artificial aerosol, infrared extinction coefficient

1. INTRODUCTION

It is known that the infrared laser technology has been developing rapidly and widely used in detecting equipment and guided weapons. That has threatened the security of potential targets. As an effective means to reduce the performance of threatening infrared aiming, reconnaissance or guidance systems, artificial aerosol has been widely used in the modern battlefields[1,2]. The artificial aerosol is composed of a large number of superfine airborne particles dispersed in the air between the protected target and the threatening infrared system. It can attenuate the intensity of the infrared energy of the target powerfully, so that the infrared reconnaissance systems cannot detect the target and recognise it. It is known that the extinction of the aerosol is dedicated to the absorption and scattering by the particles. The capability of absorption of the particles is determined by the molecular structure of the materials composing the aerosol, and the characteristic of scattering of the particle is attributed to its shape and size. To achieve the effective extinction and to make full use of the mass of the material, the ingredient, and the shape and size of the particulate should be judiciously selected[3,4]. Once the material is chosen, it is important to determine the size distribution. In this paper, the main focus is on the size designing aspect of the infrared aerosol to find the optimal particle size distribution, which provides maximum band extinction per unit mass. The particles are assumed to be small spheres. Their extinction characteristics in two infrared windows, i.e., 3~5μm and 8~14μm spectral regions have been studied.

2. EXTINCTION CHARECTERISTICS

Consider a layer of space containing a large number of small grains. A beam of electromagnetic energy illuminates the layer and penetrates it (Fig.1). So the intensity of the transmitted energy (I_t) can be written as[5]

Revised 05 June 2006

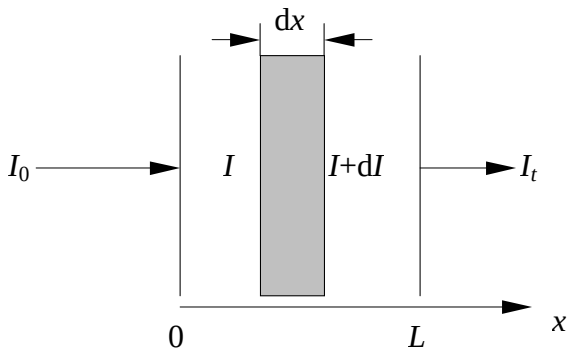

Figure 1. Change of infrared intensity when passing through the aerosol.

$$I_t = I_0 \exp[-\int_0^L \beta(\lambda) dx)] \tag{1}$$

where I_0 is the intensity of the incident energy, L is the thickness of the layer, λ is the wavelength of the electromagnetic wave, and $\beta(\lambda)$ is called the extinction coefficient. It is a parameter which describes the capability of the aerosol to attenuate the incident energy at a wavelength and it is a function of N and S. Here, N is the number density of the particles and S is called the extinction cross section of each particle. If all of the particles are of the same material and of the same size, the extinction coefficient can be written as

$$\beta(\lambda) = NS(\lambda) \tag{2}$$

When the particles are of different size, the above expression becomes:

$$\beta(\lambda) = \int_0^\infty NS(\lambda, D) f(D) dD \tag{3}$$

where $f(D)$ is the distribution function of the diameter (D) of a sphere. Because the infrared sensors generally work in a certain waveband, the parameter of an average extinction coefficient ($\overline{\beta}$), has been introduced which evaluates the ability of extinction in a waveband $\lambda_1 \sim \lambda_2$. It can be written as

$$\overline{\beta} = \frac{1}{\lambda_2 - \lambda_1} \int_{\lambda_1}^{\lambda_2} \beta(\lambda) d\lambda \tag{4}$$

Because the extinction capability of mass is of practical significance, one defines different extinctions (β_m):

$$\beta_m(\lambda) = \beta(\lambda)/\rho_0 \quad \text{and} \tag{5}$$

$$\overline{\beta}_m = \overline{\beta}/\rho_0 \tag{6}$$

where ρ_0 is the mass density of N particles, i.e.

$$\rho_0 = \int_0^\infty Nf(D)\frac{1}{6}\pi D^3 \rho \, dD \tag{7}$$

where ρ is the mass density of the particle material. According to Eqns (3),(5),(6) and (7), one gets the expression:

$$\overline{\beta}_m = \frac{1}{\lambda_2 - \lambda_1} \int_{\lambda_1}^{\lambda_2} \frac{6\int_0^\infty S(\lambda, D) f(D) dD}{\pi\rho \int_0^\infty D^3 f(D) dD} d\lambda \tag{8}$$

To calculate β_m and $\overline{\beta}_m$, one must know the expressions of $S(\lambda,D)$ and $f(D)$. $S(\lambda,D)$ is given by Mie's theory for the spherical particle:

$$S(\lambda, D) = \frac{\lambda^2}{2\pi} \sum_{n=1}^{\infty} (2n+1) \mathrm{Re}(a_n + b_n) \tag{9}$$

here

$$a_n = \frac{\varphi_n'(u)\varphi_n(x) - m\varphi_n(u)\varphi_n'(x)}{\varphi_n'(u)\xi_n(x) - m\varphi_n(u)\xi_n'(x)} \tag{10}$$

$$b_n = \frac{m\varphi_n'(u)\varphi_n(x) - \varphi_n(u)\varphi_n'(x)}{m\varphi_n'(u)\xi_n(x) - \varphi_n(u)\xi_n'(x)} \tag{11}$$

where $m = m_1 + im_2$ is the complex refractive index of the particle material, $u = mx$, $x = \pi D/\lambda$ and the prime denotes the derivative to the variable. The functions $\varphi_n(z)$ and $\xi_n(z)$ are defined as

$$\varphi_n(z) = z j_n(z) \quad \text{and} \tag{12}$$

$$\xi_n(z) = z[j_n(z) + i y_n(z)] \tag{13}$$

where j_n and y_n are the spherical Bessel functions of the first and the second kind, respectively.

As for the density distribution function $f(D)$ of the particle diameter is concerned, it can be expressed as

$$f(D) = \frac{1}{\sqrt{2\pi}\sigma D} \exp[-\frac{(\ln D - \eta)^2}{2\sigma^2}] \qquad (14)$$

in which η is the natural log of the mean, σ > 0 is the natural log of the standard deviation.

3. NUMERICAL RESULTS

Firstly, the infrared extinction coefficients of carbon, brass and hollow sphere coated with brass at different wavelengths have been calculated. The results are shown in Figs 2-4. The mass density of the carbon, brass and hollow sphere coated with brass is 0.2 g/m^3, 7.5 g/m^3 and 1.0 g/m^3, respectively, and the complex refractive indexes of carbon and brass used in the calculation are presented in Tables 1 and 2.

Table 1. Complex refractive indexes of carbon

λ (μm)	3	4	5	8	9	10	11	12	13	14
m_1	2.92	3.34	3.68	4.46	4.63	4.79	4.93	5.06	5.19	5.30
m_2	2.26	2.55	2.80	3.22	3.37	3.51	3.65	3.82	3.97	4.14

Table 2. Complex refractive indexes of brass

λ (μm)	3	4	5	8	9	10	11	12	13	14
m_1	03.23	05.08	07.10	13.38	15.05	16.88	18.88	21.00	22.87	24.98
m_2	19.10	24.70	29.90	43.30	47.50	51.60	55.60	59.50	63.00	66.80

Figure 2 shows the extinction coefficient per unit mass versus particle diameter at different wavelengths. The main features of these extinction curves are a flat response at small diameter, a maximum contribution in some diameter interval that shifts to larger sizes with longer wavelengths, and a convergence at large diameter to a common value that decreases with increasing diameter. The flat extinction at small diameter results completely from absorption. For sufficiently large particles (geometric optics limit) both scattering and absorption decrease as diameter increases and becomes independent of wavelength. Both scattering and absorption are rather large for particles with sizes comparable to the wavelength and reach the maximum at some diameter.

Similar conclusions from Figs 3 and 4 can be obtained. Moreover, Figs 2 and 3 show that the values of extinction coefficient per unit mass and the positions of maximum of the two types of materials are different. It's due to the different complex refractive indexes and different mass density of the two materials. It can be observed that the different mass density bring different extinctions as shown in Figs 3 and 4.

The above facts indicate that at different wavelengths, the size of aerosol should be different and the appropriate material should be chosen to achieve the optimal extinction.

Secondly, the average extinction coefficient of carbon in the waveband 3~5 μm and 8~14 μm has been calculated. Figures 5 and 6 show the results of an average extinction coefficient per unit mass versus mean and standard deviation of

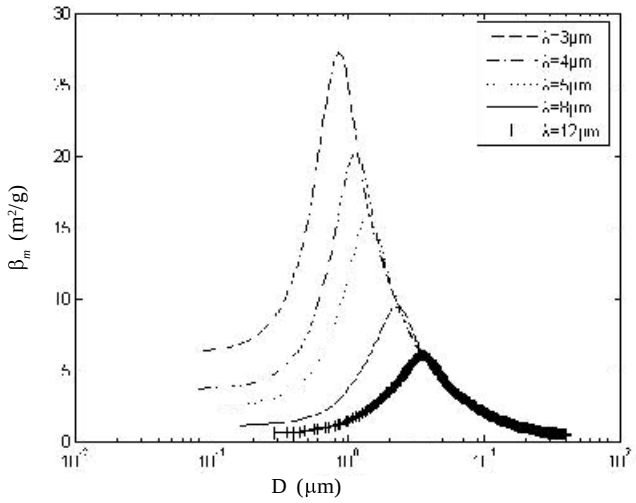

Figure 2. Extinction coefficient per unit mass versus diameter of sphere for different wavelengths of the electromagnetic wave (λ) of carbon.

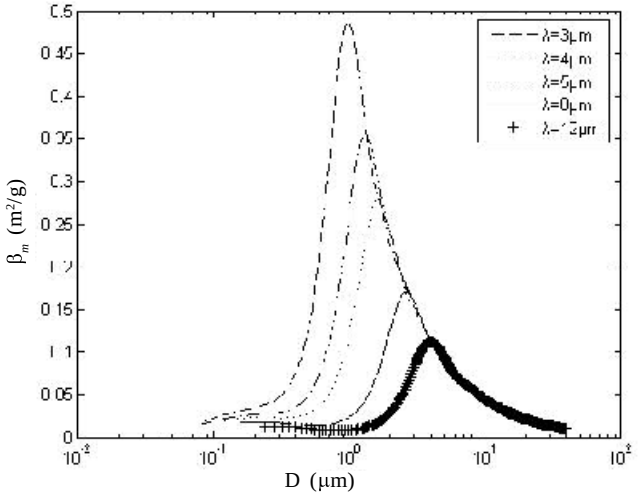

Figure 3. Extinction coefficient per unit mass versus diameter of sphere for different wavelengths of the electromagnetic wave (λ) of brass.

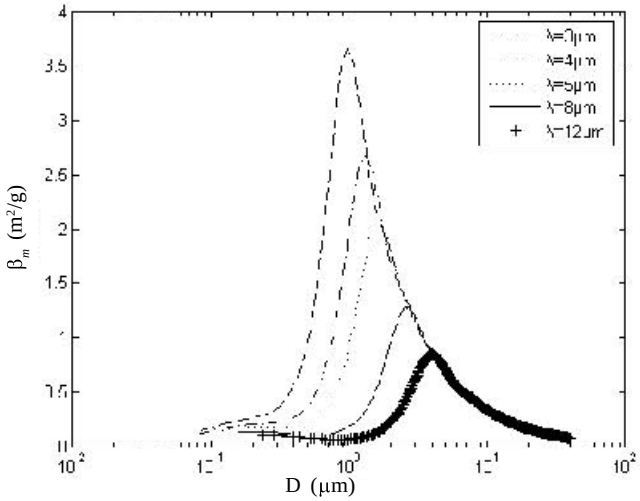

Figure 4. Extinction coefficient per unit mass versus diameter of sphere for different wavelengths of the electromagnetic wave (λ) of hollow sphere coated with brass.

ln*D* in the waveband 3~5 μm and 8~14 μm, respectively. It is found that each curve has a peak. The peaks have different locations and magnitudes. When σ grows up, the maximal extinction drops successively

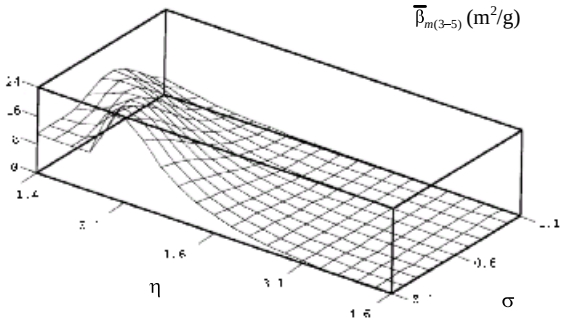

Figure 5. Average extinction coefficient per unit mass in waveband 3~5 μm versus mean and standard deviation of ln*D*.

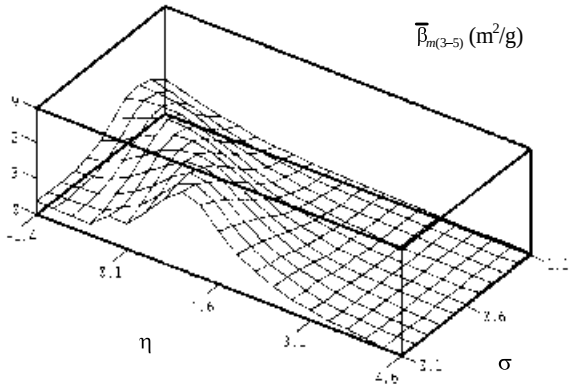

Figure 6. Average extinction coefficient per unit mass in waveband 8~14 μm versus mean and standard deviation of ln*D*.

and shifts its location to the direction of decreasing η. This means that in the range of η and σ under consideration, to obtain maximal extinction, the particle diameter has better to be close to a certain value. In the meantime, both figures show the dependence of extinction upon at given values of η. One can observe that the smaller η is, the larger σ the peak corresponds to. Figures 5 and 6 show that the trends which change with σ and η in the regions of 3~5 μm and 8~14 μm are coincident, but the values differ. This fact indicates that in different wavebands, the distribution parameters should be different to achieve the optimal extinction.

Table 3. Calculated average extinction coefficient per unit mass of carbon and hollow sphere coated with brass.

Parameters	$\overline{\beta}_{m(3-5)}$ (m²/g)	$\overline{\beta}_{m(8-14)}$ (m²/g)
Carbon (σ = 0.41, η = 2.40)	0.398	0.421
Hollow sphere coated with brass (σ = 0.41, η = 2.40)	0.250	0.265
Hollow sphere coated with brass (σ = 0.75, η = 2.00)	0.271	0.283

(a) (b)

Figure 7. Density distribution of the particle diameter used in the calculation: (a) σ = 0.41 and η = 2.40, and (b) σ = 0.75 and η=2.

Finally, the average extinction coefficients per unit mass of carbon particles and hollow spheres coated with brass with σ = 0.41 and η = 2.4 has been calculated. The average extinction coefficient of hollow spheres coated with brass with σ = 0.75 and η = 2 has also been calculated. The results are presented in Table 3. Figure 7 shows the density distribution of the particle diameter.

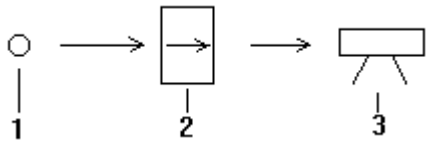

Figure 8. Schematic of the experiment: 1-infrared source, 2-smoke box, and 3-radiometer.

4. EXPERIMENTAL RESULTS AND DISCUSSION

The average extinction coefficient per unit mass of the carbon particles and two types of hollow spheres coated with brass with the double-band (3~5μm and 8~14 μm) infrared radiometer has been tested. The schematic of the experiment is shown in Fig. 8. Firstly, the radiant power of the infrared source is tested when the smoke box is empty. Secondly, the carbon particles or hollow spheres coated with brass of certain mass in the box are puffed when the infrared radiometer is working. Then, one can get the transmitted power of the infrared source. The shape of the smoke box is cubic, and its volume is 1m × 1m × 2m with 2 m in height. The extinction coefficient can be worked out with the following equation:

$$\beta(\lambda_1 \sim \lambda_2) = -\frac{\ln \dfrac{\Phi_{\lambda_1 \sim \lambda_2}(L)}{\Phi_{\lambda_1 \sim \lambda_2}(0)} V}{\rho L} \tag{15}$$

where $\Phi_{\lambda_1 \sim \lambda_2}(0)$ is the value of incident energy, $\Phi_{\lambda_1 \sim \lambda_2}(L)$ is the value of transmitted energy and L is the length of the path along which the infrared radiation travels.

The size distribution of the carbon particles used in the experiment is given by Eqn (14) with η = 2.40 and σ = 0.41. The distributions of the two types of hollow spheres coated with brass used in the experiment are described in Fig. 9, which reveals that the tested density distributions are similar to the density distributions used in the calculation.

The experimental results are shown in Figs 10-12. There are two curves in each figure. One can

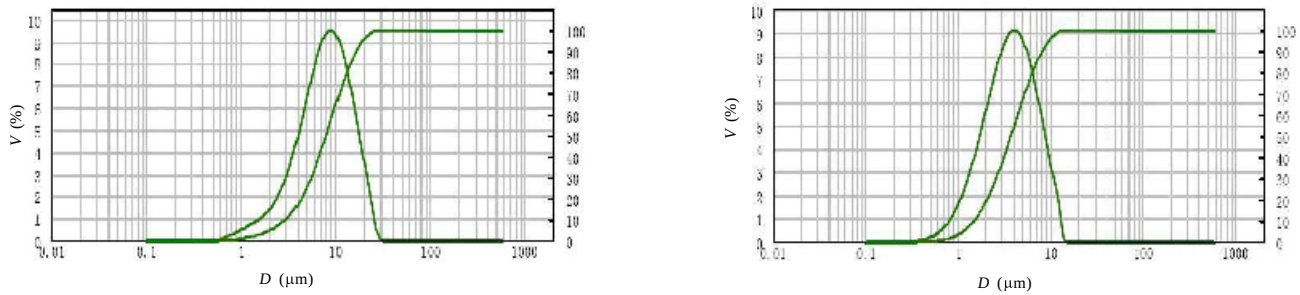

(a) (b)

Figure 9. Tested density distribution of the hollow sphere diameter coated with brass used in the experiment.

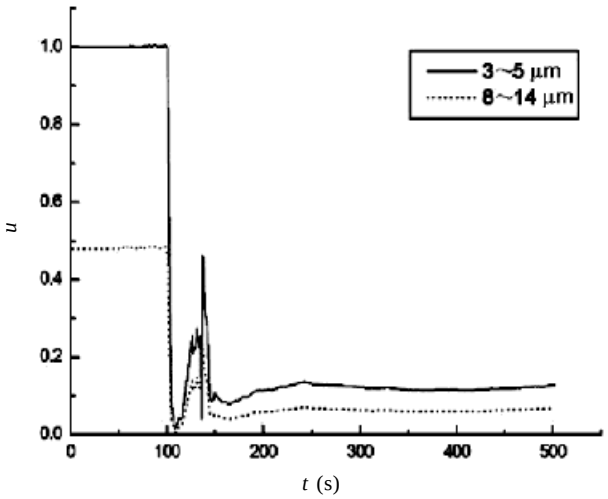

Figure 10. Transmittance curve of carbon particles.

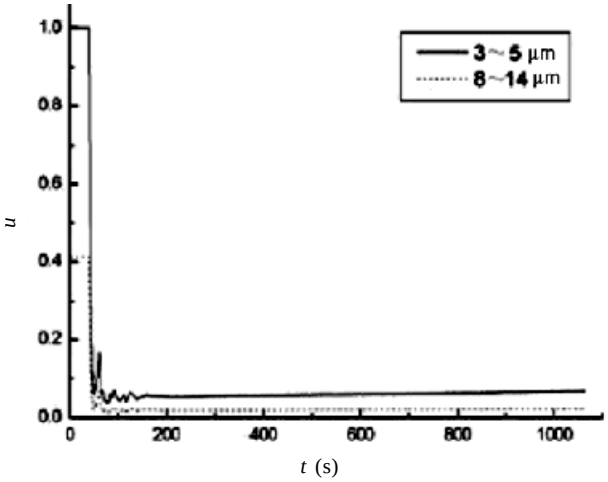

Figure 11. Transmittance curve of hollow spheres whose distribution is described by Fig. 9(a).

divide each curve into three portions. The first portion is a flat line obtained when the box is empty. When puffing the carbon particles, one get the second portion of the curve which contains one kurtosis and two valleys. It is the description of the process of screening. The third portion reflects the gradual dropping of the particles. One can calculate the extinction with the data in the initial part of the third portion.

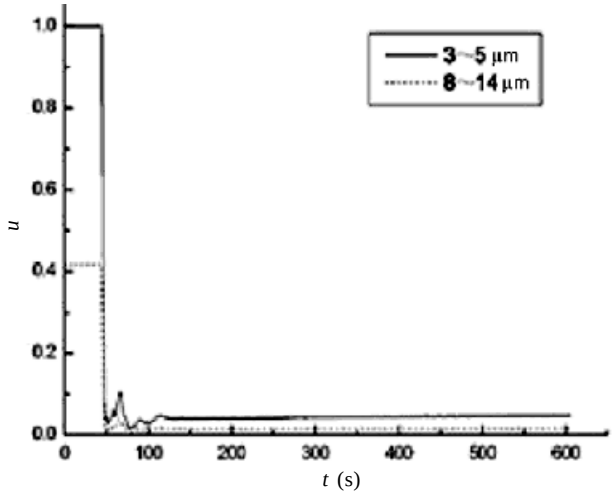

Figure 12. Transmittance curve of hollow spheres whose distribution is described by Fig. 9(b).

The tested average extinction coefficients per unit mass are shown in Table 4. Comparing the numerical results with the experimental results, one can find that the results of both carbon particles and hollow spheres coated with brass are coincident to a certain extent. The difference may be owing to that the tested particles are not absolutely spherical.

5. SUMMARY

In this paper, the application of the artificial aerosol has been discussed and the formula for studying its infrared extinction characteristics has been presented. The double-band infrared extinction coefficients of the aerosol have been calculated and compared these with the experimental data. It is assumed that the particles to be spherical with the diameter distribution being lognormal in calculating the infrared extinction coefficient of the carbon particles and two types of hollow spheres coated with brass particles.

From the numerical results, one can see that the size and complex refractive indexes of particles

Table 4. Experimental results of carbon and hollow sphere coated with brass

Parameters	$\overline{\beta}_{m(3-5)}$ (m^2/g)	$\overline{\beta}_{m(8-14)}$ (m^2/g)
Carbon	0.281	0.297
Hollow sphere coated with brass (σ = 0.41, η = 2.40)	0.370	0.390
Hollow sphere coated with brass (σ = 0.75, η = 20)	0.440	0.450

are very important to the particle's extinction capability. The results also show that at different wavebands, the size distribution parameters should be different to achieve the optimal extinction.

Comparing the numerical results with the experimental results, one can find that the numerical results of both the carbon particles and hollow spheres coated with brass coincide with the experimental results to a certain extent with the same particle size distribution parameters. The difference may be owing to that the particles used in the experiment are not absolutely spherical.

REFERENCES

1. Ladouceur, H.D. Obscurants for infrared countermeasure. NRL/FR/6111-97-9878.
2. Harris, B.L.; Shanty, F. & Wiseman, W.J. Chemical in war. *In* Kirk-Othemer Encyclopedia of Chemical Technology. Vol. 5, Ed. 3. Wiley-interscience, New York, 1979. pp. 405-08.
3. Embury, J. In search of strong infrared extinction in aerosols. *In* Proceedings of the Army Science Conference, West Point, New York, 1980.
4. Quinten, M. & Kreibig, U. Absorption and elastic scattering of light by particle aggregates. *Applied Optics*, 1993, **32**, 6173-182.
5. Jiaming, Shi; Leilei, Chen; Yongshun, Ling & Yuan, Lu. Infrared extinction of artificial aerosols and the effects of size distributions. *Inter. J. Infra. Milli. Waves*, 1998, **19**(12), 1671.

Contributors

Mr Jiachun Wang obtained his ME from the Institute of Electrical Engg., Hefei, China, in 2000. Presently, he is doing PhD (Engg). His areas of research are infrared techniques.

Mr Jiaming Shi obtained his ME from the Institute of Electrical Engineering, Hefei, China, in 1992 and the PhD (Physics) from the Institute of Plasma Physics Academy of China in 1996. His main areas of interest include: Optielectronic techniques and material science.

Mr Jiayin Wang obtained his ME from the Institute of Electrical Engineering, Hefei, China, in 2004. Presently, he is doing PhD (Engg). His main research activities include optielectronic techniques.

Mr Yongshun Ling is engaged in the research activities on optielectronic technologies.

Mr Xu Bo obtained his PhD from the Institute of Electrical Engineering, Hefei, China, in 2006. His main research field includes transmission of infrared radiation.